Delaunay Triangulation and Voronoi Diagram with Imprecise Input Data

[Extended Abstract]

A. A. Khanban
Department of Computing
Imperial College
London, U.K.
khanban@doc.ic.ac.uk

A. Edalat
Department of Computing
Imperial College
London, U.K.
ae@doc.ic.ac.uk

A. Lieutier
Dassault Systemes Provence
Aix-en-Provence & LMC/IMAG
Grenoble, France
andre_lieutier@ds-fr.com

ABSTRACT

In the framework of a new model of geometric computation, which supports the design of robust algorithms for exact real number input as well as for input with uncertainty, i.e. partial input, we show that the Delaunay triangulation and the Voronoi diagram of N computable real points in $\mathbb{R}^2$ are indeed computable. We provide a robust random incremental algorithm which, given any set of N partial inputs, i.e. N dyadic or rational rectangles in the plane, approximating these points, computes the partial Delaunay triangulation and the partial Voronoi diagram in time $O(N \log N)$. As the rectangles are refined to the N points, the sequence of partial Delaunay triangulations and the sequence of partial Voronoi diagrams converge effectively both in the Hausdorff metric and in the Lebesgue measure to the Delaunay triangulation and the Voronoi diagram of the N points respectively.

Keywords

Robust algorithm, Voronoi diagram, Delaunay triangulation, Domain theory, Imprecise points

1. INTRODUCTION

In [9], a new model for geometric computation was introduced which is based on domain theory and recursion theory, and supports a methodology for designing robust geometric algorithms in the context of exact real number inputs as well as in the framework of uncertain or imprecise input data.

In [10], this model was used to define the partial convex hull of N imprecise or partial points in $\mathbb{R}^n$ and to show that the convex hull of N computable points is indeed computable and that it can be approximated effectively by a sequence of rational (or dyadic) partial convex hulls which converge effectively to the convex hull both with respect to the Hausdorff metric and the Lebesgue measure. Furthermore, an algorithm to compute the partial convex hull was presented, which is $N \log N$ in 2d and 3d.

In this paper, we aim to tackle the problem of robustness and computability of the Delaunay triangulation and the Voronoi diagram of a finite number of points in the plane. In fact, despite a great number of algorithms and articles published on robustness issues related to the Delaunay triangulation and the Voronoi diagram of a finite number of points in the plane [28, 12, 27, 21, 1, 5], the question of computability of the Delaunay triangulation and the Voronoi diagram for general exact real number inputs or the problems of computing the Delaunay triangulation and the Voronoi diagram for imprecise input points have not been previously addressed.

Robustness problems arise from the discrepancy between the unrealistic real RAM machine model [24], used to prove the correctness of algorithms, and real computers which are only able to deal with finite data. Mathematically correct algorithms in this model, when implemented in floating point arithmetic, become unreliable and lead to inconsistencies and potentially disastrous results. These inconsistencies are consequence of numerical errors in evaluating the predicates in the combinatorial, i.e. the symbolic, logical or topological, part of geometric algorithms. The problem is related to the fact that, while basic arithmetic operators and analytic functions on real numbers are Turing-computable, comparison of two real numbers is only semi-decidable [29].

Non-robustness issues are particularly serious in computational geometry in which combinatorial computations usually rely on numerical ones: small numerical inaccuracies turn into fatal inconsistencies in the combinatorial part of the computation.

For example in the problem of Delaunay triangulation depicted in Figure 1, the effect of a small perturbation changing the point t to t' makes the previously legal edge vr illegal, while the previously illegal edge ut now becomes the legal edge ut'.

Computing with uncertain inputs is unavoidable in physical modelling [6, 22]. In applications such as robotics or solid modelling, actual geometric inputs are measurements

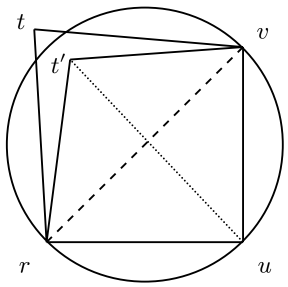

Figure 1: Effect of imprecise input in Delaunay triangulation.

of physical objects, and as such, they are inherently uncertain and can only be represented for example using intervals of numbers.

In brief, one can classify existing approaches to robustness into two main categories. The first is the so-called exact computation model. It is based on simulating a real RAM by restricting real computations to a countable subfield of $\mathbb{R}$, usually the rational numbers or a subfield of algebraic numbers [7, 3, 4, 13, 2, 14, 30, 19] for which the comparison predicate is computable. The second category, as for example in ϵ-geometry [16] or in interval geometry [25, 18, 17], tries to devise correct predicates from imprecise data and computations [26, 20].

Since the output of an algorithm often may have to be used again as the input of a new one, the depth of computation can be a priori unknown. In such cases, even in the exact methods, some form of *rounding*, with loss of information, to prevent an unrealistic growth in the size of the data is unavoidable [15].

Our new approach, which may be put in the second category, provides a general model of computation in which provably correct algorithms match naturally with feasible programs.

In this paper, aimed at the computational geometry community, we focus on practical algorithms and will only briefly describe the underlying mathematical model given in [9] that relies on recursion theory and domain theory [23, 8, 11]. We illustrate our model of computation for the non-continuous, and hence non-computable, sign predicate $s : \mathbb{R} \to \{-, 0, +\}$ that gives the sign of a real number.

In order to define the best Turing-computable approximation of this predicate, we first introduce the set $\mathbf{I}\mathbb{R}$ of real intervals. The *information order* $\sqsubseteq$ on real intervals is reverse inclusion: $[a, b] \sqsubseteq [c, d] \iff_{\text{def}} [a, b] \supseteq [c, d]$. Thus, $[a, b] \sqsubseteq [c, d]$ means that $[c, d]$ refines (or has more information than) the information given by $[a, b]$. The partial order $\mathbf{I}\mathbb{R}$ is a *complete partial order* (*cpo* or *domain*), i.e. every directed set (in particular every increasing sequence) has a supremum, namely the intersection of all the compact intervals in the directed set. The set $\mathbb{D}$ of dyadic numbers is the set of rational numbers whose denominator is a power of 2, in other words, whose binary expansion is finite. A dyadic interval is a closed interval whose ends are dyadic numbers. The countable set $\mathbf{I}\mathbb{D}$ of dyadic intervals, is said to form a *basis* of $\mathbf{I}\mathbb{R}$. Alternatively, we can work with the basis $\mathbf{I}\mathbb{Q}$ of rational intervals.

The supremum of an increasing[1] sequence of dyadic intervals is a real interval, namely the intersection of all the dyadic intervals in the sequence. The maximal real intervals $[x, x]$ are identified with real numbers. A real interval $[a, b]$ is *computable* if there is an *effective* increasing sequence of basis elements whose supremum (i.e. intersection) is $[a, b]$, i.e. there is a program which with input n outputs the n^{th} element of the sequence of basis elements.

For an interval $[a, b]$, define the sign predicate:

$$s([a,b]) = \begin{cases} - & \text{if } b < 0, \\ \perp & \text{if } a \leq 0 \leq b, \\ + & \text{if } a > 0. \end{cases} \tag{1}$$

Here $\perp$ stands for "any value from $\{-, 0, +\}$" and the range of s is the three element partial order $\{-, +, \perp\}$, which is denoted by $\{-, +\}_\perp$ in which $+$ and $-$ are incomparable and $\perp$ is the least element.

In our model, a real number x is given by an infinite increasing sequence of dyadic intervals x_k. Applying (1) to each x_k would give a sequence b_k of combinatorial (boolean) answers which converge in $\{-, +\}_\perp$. The sign predicate is Scott continuous[2] and an implementation of this predicate would consist in computing (1) on dyadic intervals which is possible on an integer RAM machine.[3]

In subsequent sections, we apply this model of computation to the problem of computing the Delaunay triangulation and the Voronoi diagram of N elements of $\mathbf{I}\mathbb{R}^2$. The set $\mathbf{I}\mathbb{D}^2$ (or $\mathbf{I}\mathbb{Q}^2$) of all rectangles with dyadic (or rational) vertices, is a basis for the domain $\mathbf{I}\mathbb{R}^2$, which simply means that any real rectangle in the plane is the intersection of a nested shrinking sequence of dyadic (or rational) rectangles. Using the same scheme as for the sign predicate, it is enough to compute the Delaunay triangulation and the Voronoi diagram for a set of N dyadic (or rational) rectangles, i.e. elements in $\mathbf{I}\mathbb{D}^2$ (or $\mathbf{I}\mathbb{Q}^2$).

In our framework, geometric objects, i.e. subsets of $\mathbb{R}^d$, are captured by elements of the *solid domain* $\mathbf{S}\mathbb{R}^d$, which are called *partial solids* or *partial geometric objects* [9]. A geometric object is represented by a pair (I, E) of disjoint open sets, representing respectively the interior I and the exterior[4] E of the object. The information ordering is componentwise inclusion, i.e. $(I, E) \sqsubseteq (I', E')$ iff $I \subseteq I'$ and

[1] i.e. increasing with respect to the information order $\sqsubseteq$.

[2] A monotone (i.e. information order preserving) map f between cpo's is *Scott continuous*, if for any increasing sequence x_n, we have $f(\sup_{n \geq 0}(x_n)) = \sup_{n \geq 0}(f(x_n))$. Thus, it is enough to compute f on basis elements to obtain an algorithm that computes approximations which converge to $f(x)$ for any x.

[3] In this paper, we assume a machine model of computation a RAM (Random Access Memory) machine able to perform usual integer (and hence rational and dyadic) arithmetic. As regards computability, this machine model is equivalent to a universal Turing machine.

[4] The exterior of a set is the interior of its complement.

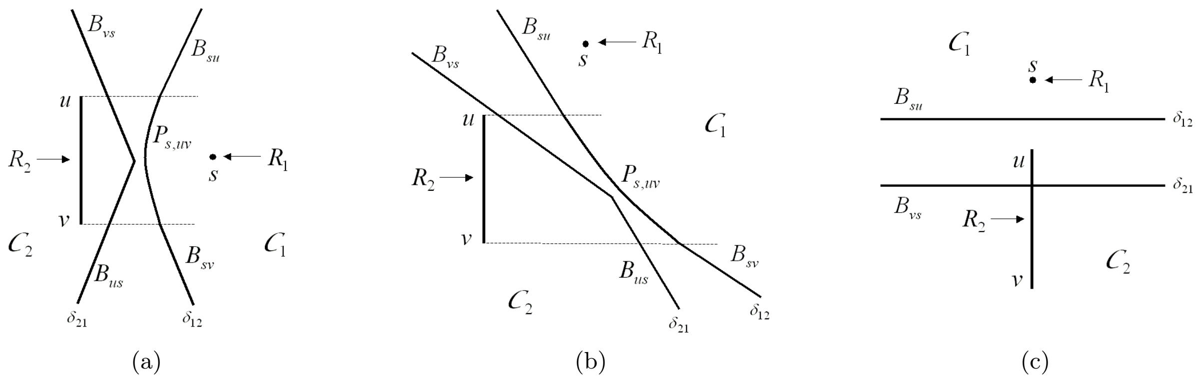

Figure 2: Partial Voronoi diagram of one point and a line segment.

$E \subseteq E'$. The geometric object (I, E) is maximal in $\mathbf{S}\mathbb{R}^d$ iff $I = (E^c)^\circ$ and $E = (I^c)^\circ$, where X° and X^c denote respectively the interior and the complement of a set X. The collection of pairs of interiors of dyadic (or rational) polytopes forms a basis for $\mathbf{S}\mathbb{R}^d$. Any geometric object (I, E) can be obtained as the union of these basis elements. And (I, E) is *computable* if there exists an increasing effective sequence of these basis elements with union (I, E).

2. PARTIAL VORONOI DIAGRAM

The problem of computing the Voronoi diagram of N partial points, i.e. N compact rectangles in the plane can be stated as follows. For a point $x \in \mathbb{R}^2$ and a compact rectangle $R \subset \mathbb{R}^2$, let $d_s(x, R) = \min\{|x - y| : y \in R\}$ and $d_l(x, R) = \max\{|x - y| : y \in R\}$ be, respectively, the shortest and longest distance from x to R. Now consider two rectangles R_i and R_j. The *interior of the Voronoi cell of R_i with respect to R_j* is given by $\mathcal{C}_{ij} = \{x \in \mathbb{R}^2 \mid d_l(x, R_i) < d_s(x, R_j)\}$. The *exterior of the Voronoi cell of R_i with respect to R_j* is given by $\mathcal{C}_{ji} = \{x \in \mathbb{R}^2 \mid d_l(x, R_j) < d_s(x, R_i)\}$. Note that interiors and exteriors are dual with respect to R_i and R_j: the interior of the Voronoi cell of R_j with respect to R_i is the exterior of the Voronoi cell of R_i with respect to R_j and vice versa.

The *interior of the Voronoi cell* of R_i is defined to be the set of points which are closer to any point in R_i than to any point in R_j $(j \neq i)$. More precisely, $\mathrm{Int}(\mathcal{C}_i) = \{x \in \mathbb{R}^2 \mid \forall j \neq i;\ d_l(x, R_i) < d_s(x, R_j)\}$. The exterior of the Voronoi cell of R_i is defined to be the set $\mathrm{Ext}(\mathcal{C}_i) = \{x \in \mathbb{R}^2 \mid \exists j \neq i;\ d_l(x, R_j) < d_s(x, R_i)\}$. Thus, we have

$$\mathrm{Int}(\mathcal{C}_i) = \bigcap_{j \neq i} \mathcal{C}_{ij} \quad \text{and} \quad \mathrm{Ext}(\mathcal{C}_i) = \bigcup_{j \neq i} \mathcal{C}_{ji}.$$

Note that, even in the case that we only have line segments, the problem we address here is very different from the well-known problem referred to as "line segment Voronoi diagram" [1], which takes line segments as sites and considers the shortest distance to these segments. This is already illustrated in the simplest non-trivial case in Figure 2: there are only two rectangles R_1 and R_2 where R_1 is a degenerate rectangle containing only one point s and R_2 is a degenerate rectangle consisting of the vertical line segment uv, with $s \notin uv$. In this case, we have only two partial points, so $\mathcal{C}_1 = \mathcal{C}_{12}$ and $\mathcal{C}_2 = \mathcal{C}_{21}$. In Figures 2(a) and 2(b), where s, u and v are not collinear, the boundary of $\mathcal{C}_1$, namely $\delta_{12} = \{x \in \mathbb{R}^2 \mid d_l(x, R_1) = d_s(x, R_2)\}$, consists of the following three parts:

(i) the semi-infinite line B_{su}, part of the PB (Perpendicular Bisector) of su,

(ii) the segment $P_{s,uv}$ of the parabola with focus s and directrix passing through u and v,

(iii) the semi-infinite line B_{sv}, part of the PB of sv.

In the "line segment Voronoi diagram", δ_{12} is the boundary of the cell of R_1 and that of R_2, and provides the complete diagram. But in the new model we still need to find $\mathcal{C}_2$ whose boundary, $\delta_{21} = \{x \in \mathbb{R}^2 \mid d_l(x, R_2) = d_s(x, R_1)\}$, is different from δ_{12} and consists of the semi-infinite line B_{us}, part of the PB of us, and the semi-infinite line B_{vs}, part of the PB of vs. In Figure 2(c), that s, u and v are collinear, δ_{12} is the line B_{su} and δ_{21} is the line B_{vs}.

Note that even in this simple example the boundaries of the two regions do not coincide. In fact, the open region bounded by the two boundaries consists of points which are indeterminate, i.e. with the information available one cannot determine if they are in $\mathcal{C}_1$ or in $\mathcal{C}_2$. In terms of our model, $\mathcal{C}_1$ is the interior of the partial Voronoi cell of R_1 whereas $\mathcal{C}_2$ is the exterior of the partial Voronoi cell of R_1 (and vice versa for the partial Voronoi cell of R_2). If the input information is refined, i.e. if the line segment uv is shrunk, then some of the indeterminate points will fall in $\mathcal{C}_1$, i.e. the interior of R_1 expands, and some of the indeterminate points will fall in $\mathcal{C}_2$, i.e. the exterior of R_1 expands as well. In the limit when uv shrinks to a single point c, say, then the two boundaries tend to the PB of sc and we are in the classical case.

It is well known that, classically, the problem of the Voronoi diagram of a finite number of points in the plane can be reduced to computing the Delaunay triangulation of the set of points [5, 12]. We will see that the Voronoi diagram of a finite number of partial points, i.e. rectangles in the plane, can also be computed from a Delaunay triangulation of these partial points. Recall that three points of a given set of points in the plane form a Delaunay triangle if and

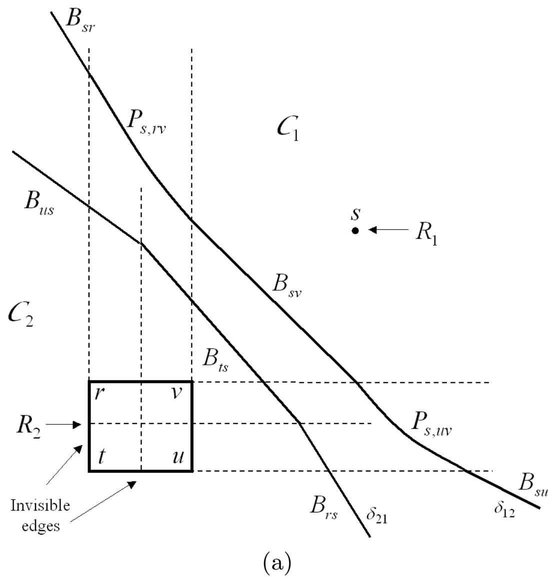

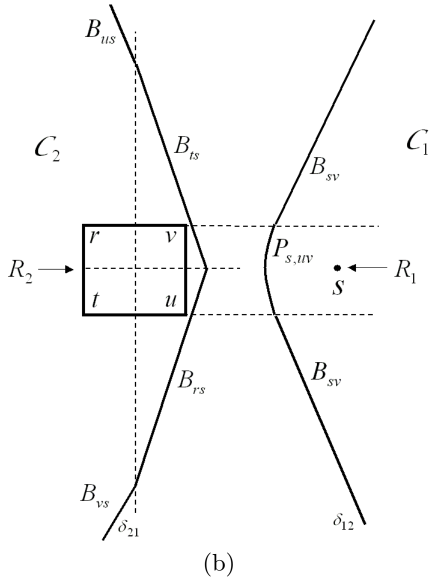

Figure 3: Partial Voronoi diagram of one point and a rectangle.

only if their circumcircle does not contain any points of the set in its interior. The centre of the circumcircle is at the intersection point of the PB's.

We will see that in analogy with the classical case, the "partial Delaunay triangulation" of a finite set of partial points in the plane can be computed by determining the "partial circles" of the triples of partial points which do not contain any partial point in their interior. The "partial centre" of the partial circle passing through three partial points is computed by obtaining the intersection of the "partial PB's" of the three "partial edges".

3. PARTIAL PERPENDICULAR BISECTOR

The *partial PB* map is formally given by

$$\begin{array}{rccc} \mathcal{B}: & \mathbf{I}\mathbb{R}^2 \times \mathbf{I}\mathbb{R}^2 & \to & \mathbf{S}\mathbb{R}^2 \\ & (R_1, R_2) & \mapsto & (\emptyset, \mathcal{C}_1 \cup \mathcal{C}_2), \end{array}$$

where $\mathcal{C}_1$ and $\mathcal{C}_2$ are the interiors of the partial Voronoi cells of R_1 and R_2 respectively, as defined in Section 2. Since the interior of the partial PB is always empty, we can identify $\mathcal{B}(R_1, R_2)$ with the closed set $(\mathcal{C}_1 \cup \mathcal{C}_2)^c$, where A^c denotes the complement of A. In the rest of the paper we therefore take:

$$\begin{array}{l} \mathcal{B}(R_1, R_2) = (\mathcal{C}_1 \cup \mathcal{C}_2)^c = \\ \{z \in \mathbb{R}^2 \mid \exists x \in R_1,\ y \in R_2;\ |z - x| = |z - y|\}. \end{array} \qquad (2)$$

What does $\mathcal{B}(R_1, R_2)$ look like in general? To see this, it is convenient to first obtain $\mathcal{C}_1$ for the case where R_1 is a degenerate rectangle consisting of a single point s and R_2 is a general rectangle. Clearly if $s \in R_2$ then $\mathcal{B}(R_1, R_2) = \mathbb{R}^2$. Otherwise, the boundary of $\mathcal{C}_1$ is depicted in Figure 3(a) for the case that s lies outside the closed vertical and horizontal strips induced by R_2. We see that the boundary δ_{12} of $\mathcal{C}_1$ is given by the line segment B_{sv}, part of the PB of sv, the two semi-infinite line segments B_{su} and B_{sr} and finally the two parabolic segments $P_{s,uv}$ and $P_{s,rv}$. Note that the two edges rt and tu are invisible from s and thus make no contribution to the boundary of $\mathcal{C}_1$. The boundary δ_{21} of $\mathcal{C}_2$ consists of one line segment B_{ts} and two semi-infinite line segments B_{us} and B_{rs}.

If s lies, say, on the horizontal strip of R_2 on the side of uv, then δ_{12} will be as in Figure 2(a). And δ_{21} will consist of two line segments B_{rs} and B_{ts} and two semi-infinite line segments B_{us} and B_{vs}, as depicted in Figure 3(b).

Proposition 1. *The Voronoi cell of a point with respect to a rectangle is the intersection of the Voronoi cells of the point and the visible edges of the rectangle.*

Proposition 2. *The Voronoi cell of a rectangle with respect to another rectangle is the intersection of the Voronoi cells of the vertices of the rectangle with respect to the other rectangle.*

Based on these results, we can determine the cells $\mathcal{C}_1$ and $\mathcal{C}_2$ of two non-intersecting but otherwise arbitrary compact rectangles R_1 (with vertices x, y, z, w) and R_2 (with vertices u, v, r, t) as shown in Figure 4, where we have assumed that the horizontal strips induced by R_1 and R_2 do not intersect, similarly for the vertical strips.

The interior $\mathcal{C}_{R_1 R_2}$ of the partial Voronoi cell of R_1 is the intersection of the four interiors of the partial Voronoi cells $\mathcal{C}_{xR_2}$, $\mathcal{C}_{yR_2}$, $\mathcal{C}_{zR_2}$, and $\mathcal{C}_{wR_2}$. The boundaries of each of these open regions has, as we have just seen, three linear and two parabolic segments. The boundary δ_{12} of the intersection of the four interiors has seven linear and parabolic segments, which, as in Figure 4, are given by B_{xr}, $P_{x,rv}$, $P_{y,rv}$, B_{yv}, B_{zv}, $P_{z,uv}$ and B_{zu}. A similar boundary δ_{21} is obtained for the interior $\mathcal{C}_{R_2 R_1}$ of the partial Voronoi cell of R_2.

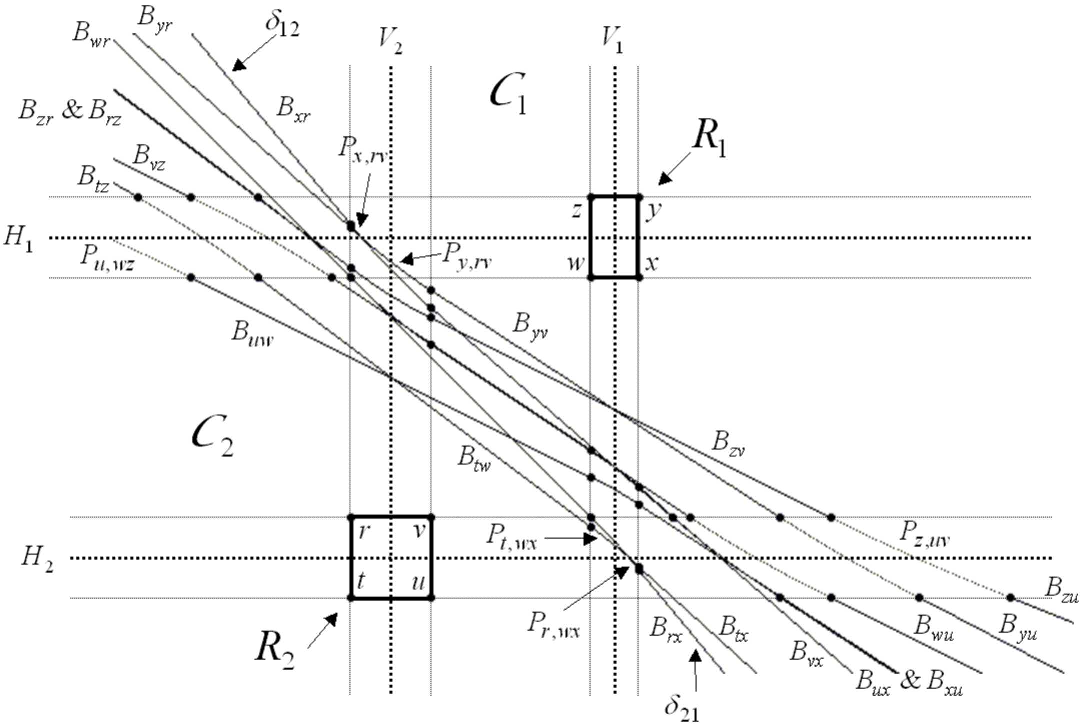

Figure 4: Partial Voronoi diagram of two rectangles.

Indeed, we can exactly identify which part of δ_{12} comes from the boundaries of $\mathcal{C}_{xR_2}$, $\mathcal{C}_{yR_2}$, $\mathcal{C}_{zR_2}$ and $\mathcal{C}_{wR_2}$. The horizontal line H_1 and the vertical line V_1 passing through the centre of R_1 divide the plane into four regions. In each region, δ_{12} is part of the boundary of $\mathcal{C}_{sR_2}$, where s is the vertex in the diagonally opposite region. For example, in Figure 4, the semi-infinite line B_{xr} and a segment of $P_{x,rv}$ form the part of δ_{12}, which comes from the boundary of $\mathcal{C}_{xR_2}$. On the horizontal line H_1, δ_{12} changes from $P_{x,rv}$ to $P_{y,rv}$, which comes from the boundary of $\mathcal{C}_{yR_2}$ and continues with B_{yv}. On the vertical line V_1, δ_{12} changes from B_{yv} to B_{zv}, which comes from the boundary of $\mathcal{C}_{zR_2}$ and continues with $P_{z,uv}$ and the semi-infinite line B_{zu}.

Note that no part of the boundary of $\mathcal{C}_{wR_2}$ is used in δ_{12}, and no part of the boundary of $\mathcal{C}_{vR_1}$ is used in δ_{21}. This always happens when R_1 and R_2 do not intersect the horizontal and vertical strips of each other.

4. PARTIAL DISC

We can now compute the partial disc whose boundary goes through three given partial points. For three non-collinear points $x, y, z \in \mathbb{R}^2$, let D_{xyz} be the unique closed disc whose boundary circle passes through x, y and z. Formally, we define the partial disc map by:

$$\begin{array}{rccc} \mathcal{D}: & (\mathbf{I}\mathbb{R}^2)^3 & \to & \mathbf{S}\mathbb{R}^2 \\ & (R_1, R_2, R_3) & \mapsto & (I, E), \end{array}$$

where $I = E = \emptyset$ if there exists a straight line which intersects R_1, R_2 and R_3, otherwise $I = (\bigcap\{D_{xyz} \mid x \in R_1,\ y \in R_2,\ z \in R_3\})^\circ$ and $E = (\bigcup\{D_{xyz} \mid x \in R_1,\ y \in R_2,\ z \in R_3\})^c$.

We will now describe how to compute $I = I(R_1, R_2, R_3)$ and $E = E(R_1, R_2, R_3)$. We assume that R_1, R_2, R_3 satisfy the non-collinearity condition, namely that there exists no straight line which intersects all three rectangles. Then the intersection $\mathcal{O}(R_1, R_2, R_3) = \mathcal{B}(R_1, R_2) \cap \mathcal{B}(R_2, R_3) \cap \mathcal{B}(R_1, R_3)$ will in general be a compact set whose boundary consists of six vertices with six straight line and parabolic segments from δ_{12}, δ_{21}, δ_{13}, δ_{31}, δ_{23} and δ_{32} (Figure 5).

Proposition 3. $\mathcal{O}(R_1, R_2, R_3) = \{s \in \mathbb{R}^2 \mid \exists x \in R_1, y \in R_2, z \in R_3; |x - s| = |y - s| = |z - s|\}$.

Using the above proposition, we can say that $\mathcal{O}(R_1, R_2, R_3)$ is the locus of centres of circles which intersect R_1, R_2 and R_3; we call it the *partial centre* of the partial circumcircle of the three partial points. The vertices are given by

$$\begin{array}{ll} o_{CFC} = \delta_{21} \cap \delta_{23}, & o_{FCF} = \delta_{12} \cap \delta_{32}, \\ o_{CFF} = \delta_{21} \cap \delta_{31}, & o_{CCF} = \delta_{31} \cap \delta_{32}, \\ o_{FFC} = \delta_{13} \cap \delta_{23}, & o_{FCC} = \delta_{12} \cap \delta_{13}. \end{array}$$

Note that o_{CCF} is the centre of a circle with radius r_{CCF} which passes through (i) the point of R_1 closest to o_{CCF}, (ii) the point of R_2 closest to o_{CCF} and (iii) the point of R_3 furthest from o_{CCF}; hence the subscript in o_{CCF}. Similarly for the other vertices. If any one or more of the rectangles R_1, R_2 and R_3 are in fact singletons then some of these vertices coincide.

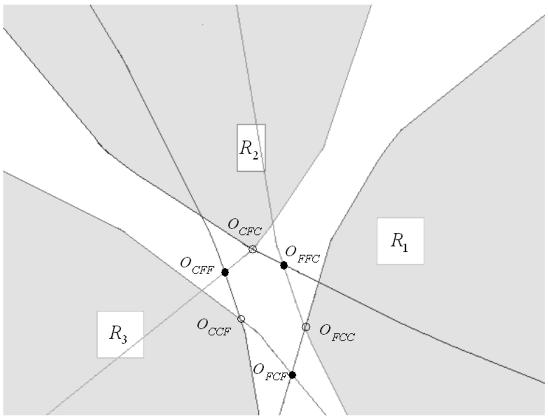

Figure 5: Partial Voronoi diagram of three rectangles.

PROPOSITION 4. *The set of vertices of the partial centre consists of the points o_{CCF}, o_{CFC}, o_{CFF}, o_{FCC}, o_{FCF} and o_{FFC}. If none of R_1, R_2 and R_3 is a singleton then the above six points are distinct. If R_1 is a singleton but not R_2 and R_3 then $o_{CFC} = o_{FFC}$ and $o_{CCF} = o_{FCF}$ and other points are distinct. If only R_1 and R_2 are singletons then we have two distinct points $o_{CFC} = o_{FCC} = o_{FFC}$ and $o_{CCF} = o_{CFF} = o_{FCF}$.*

Let $D(x, r)$ denote the closed disc with centre x and radius r. Consider the three discs $D_1 = D(o_{FCC}, r_{FCC})$, $D_2 = D(o_{CFC}, r_{CFC})$ and $D_3 = D(o_{CCF}, r_{CCF})$ on the one hand and the three discs $D'_1 = D(o_{CFF}, r_{CFF})$, $D'_2 = D(o_{FCF}, r_{FCF})$ and $D'_3 = D(o_{FFC}, r_{FFC})$ on the other hand.

THEOREM 1. *The interior and the exterior of the partial disc $(I(R_1, R_2, R_3), E(R_1, R_2, R_3)) = \mathcal{D}(R_1, R_2, R_3)$ are given by:*

$$I(R_1, R_2, R_3) = (D_1 \cap D_2 \cap D_3)^\circ$$
$$E(R_1, R_2, R_3) = (D'_1 \cup D'_2 \cup D'_3)^c.$$

In Figure 6, the boundaries of the discs D_1, D_2 and D_3 are depicted with dotted lines, those of D'_1, D'_2 and D'_3 with solid lines and the boundaries of the sets I and E with dashed lines. The closed region bounded between I and E, i.e. bounded between the two closed dashed curves, is called the *boundary of the partial disc.*

Using the above theorem, one can show:

THEOREM 2. *The partial disc map $\mathcal{D}$ is Scott continuous (i.e. it preserves the partial order and the supremums of directed sets) and is computable (i.e. it sends any computable sequence of basis elements of $(\mathbf{I}\mathbb{R}^2)^3$ to a computable sequence of partial discs in $\mathbf{S}\mathbb{R}^2$.*

Now assume that the three rectangles $R_1 = \{p_1\}$, $R_2 = \{p_2\}$ and $R_3 = \{p_3\}$ are actually singletons, and that p_1, p_2 and

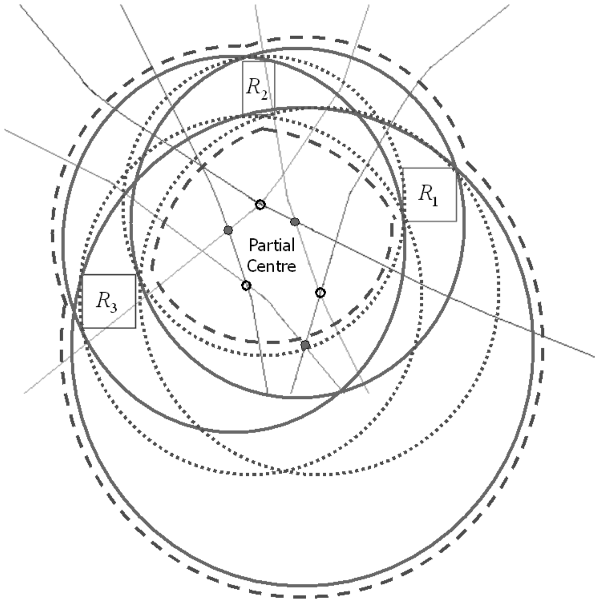

Figure 6: The interior and exterior of a partial disc.

p_3 are computable non-collinear points of $\mathbb{R}^2$ which are approximated by three computable sequences of dyadic (or rational) rectangles: $\{p_i\} = \bigcap_{j\geq 0} R_{ij}$, for $i = 1, 2, 3$. We have the following results. The two increasing sequences of open sets $(I(R_{1j}, R_{2j}, R_{3j}))_{j\geq 0}$ and $(E(R_{1j}, R_{2j}, R_{3j}))_{j\geq 0}$ converge respectively to the interior and the exterior of the disc $D_{p_1p_2p_3}$, which form a maximal element of $\mathbf{S}\mathbb{R}^d$. Moreover, this convergence is *effective* in the Hausdorff distance and Lebesgue measure, which means, in particular, that there is an algorithm that, given an integer m as input, can compute n such that whenever $j \geq n$ the Hausdorff distance (respectively the volume, or Lebesgue measure of the set-theoretic difference) between $D_{p_1p_2p_3}$ and $\overline{I(R_1, R_2, R_3)}$ is bounded by 2^{-m} (and a similar relation on the exterior, E).

We now define the *containment* predicate

$$\mathrm{Con} : \mathbf{I}\mathbb{R}^2 \times (\mathbf{I}\mathbb{R}^2)^3 \to \{+, -\}_\perp$$
$$(R, (R_1, R_2, R_3)) \mapsto \begin{cases} + & \text{if } R \subset I(R_1, R_2, R_3) \\ - & \text{if } R \subset E(R_1, R_2, R_3) \\ \perp & \text{otherwise.} \end{cases}$$

Then it can be shown that Con is Scott continuous and is decidable on basis elements, which means that if the input $(R, (R_1, R_2, R_3))$ is a tuple of dyadic (or rational) rectangles, then we can decide in finite time if Con is true or false ($+$ or $-$) for this input. From this it will follow that Con is computable, i.e. given a computable tuple $(R, (R_1, R_2, R_3))$, then in *finite* time, i.e. by looking at only a finite number of the elements of the four sequences of basis elements approximating R and (R_1, R_2, R_3), we can verify that R is contained in the interior partial disc I or in the exterior partial disc E, i.e. containment in the interior and exterior of the partial circle is semi-decidable.

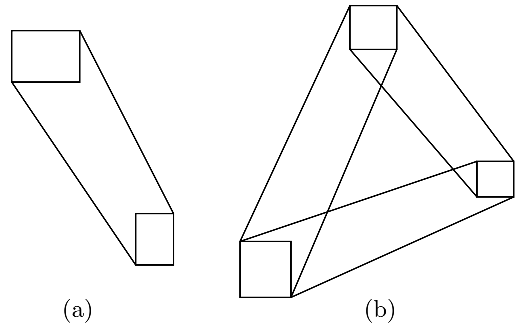

Figure 7: Partial edge (a) and partial triangle (b).

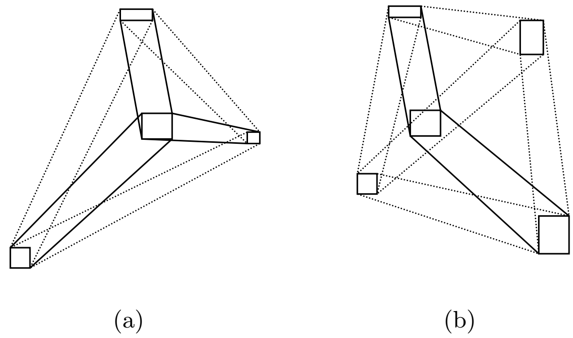

Figure 8: New partial point is in the interior (a) or intersects the boundary (b) of a partial triangle.

5. PARTIAL DELAUNAY TRIANGULATION

Suppose we are given N dyadic rectangles $R_1 \cdots R_N$ in the plane. Given any i_1, i_2, i_3, i_4 with $1 \leq i_1, i_2, i_3, i_4 \leq N$, we can use the decidable predicate Con on dyadic rectangles to determine if $R_{i_4} \subset I(R_{i_1}, R_{i_2}, R_{i_3})$ or if $R_{i_4} \subset E(R_{i_1}, R_{i_2}, R_{i_3})$.

PROPOSITION 5. *Suppose four rectangles are given, any three of which satisfy the non-collinearity condition.*

(i) If one of the rectangles intersects the boundary of the partial disc of the other three rectangles, then any of the rectangles intersects the boundary of the partial disc of the other three rectangles.

(ii) If one of the rectangles is in the interior of the partial disc of the other three rectangles, then one of these three rectangles is in the exterior of the partial disc of the other three rectangles.

We define a partial edge between two partial points (closed rectangles) R_1 and R_2 to be the convex hull of R_1 and R_2, written $\mathrm{Ed}(R_1, R_2)$. We can also define a partial triangle to be the partial convex hull of three partial points (Figure 7).

Now that we have defined partial points, partial edges, partial triangles and partial discs, we apply the classical random incremental algorithm for Delaunay triangulation [5], using Con instead of the classical predicate for containment of a point in the interior of a disc, for partial objects.

The algorithm is randomized incremental, so it adds the partial points in random order and it maintains a partial Delaunay triangulation of the current partial point set. Consider the addition of a partial point. If this partial point is in the interior of a partial triangle, then we add three new partial edges from this partial point to the three partial vertices of the triangle (Figure 8a). On the other hand, if the new partial point intersects the boundary of a partial triangle, which would be a sharing partial edge of two neighbouring partial triangles, we add two new partial edges by connecting the new partial point to the two opposite vertices of this edge in these two neighbouring partial triangles (Figure 8b). Then we start the process of flipping illegal partial edges to legal partial edges. By part (i) of Proposition 5, we know that not with standing the order we insert the new partial points, the result will be the same. By part (ii) of Proposition 5, it follows that when we flip an illegal partial edge we obtain a legal one.

Note that if the boundary of the partial disc of three rectangles intersects other rectangles, then the question of legality of the edges between the rectangles on the opposite side of the circle remains indeterminate at the present level of precision, a feature which is similar to the classical case when the circumcircle of a triangle contains a fourth point on its boundary. While some edges may remain indeterminate at a given stage of computation, the strength of the method lies in detecting those edges which are definitely legal or definitely illegal, so that the right choice can be made. Since computing Con takes $O(1)$ time, we thus obtain an algorithm to determine a partial Delaunay triangulation in average time $O(N \log N)$ as in the classical algorithm.

This gives us the partial Delaunay triangulation map:

$$\begin{array}{rcl} \mathcal{T}: \quad (\mathbf{I}\mathbb{R}^2)^N & \to & \mathbf{S}\mathbb{R}^2 \\ \mathcal{T}(R_1, \ldots, R_N) & = & (\emptyset, (\bigcup\{\mathrm{Ed}(R_i, R_j) \mid \\ & & \mathrm{Ed}(R_i, R_j) \text{ legal or indeterminate}\})^c). \end{array}$$

THEOREM 3. *The partial Delaunay triangulation map $\mathcal{T}$ is Scott continuous and Hausdorff and Lebesgue computable.*

We can then use our partial Delaunay triangulation to compute the partial Voronoi diagram on dyadic (or rational) rectangles. By determining the partial PB's of the legal pairs of partial points which are of order $O(N)$, we then obtain $\mathrm{Int}(\mathcal{C}_i)$ for $1 \leq i \leq N$, giving the partial Voronoi diagram of the N partial points in time $O(N \log N)$.

We finally discuss the question of computability of the Voronoi diagram in detail. We define the partial Voronoi map on a list of N rectangles in the plane:

$$\mathcal{V} : (\mathbf{I}\mathbb{R}^2)^N \to (\mathbf{S}\mathbb{R}^2)^N,$$

with the ith component, $1 \leq i \leq N$, defined as

$$\mathcal{V}_i : (R_j)_{1 \leq j \leq N} \mapsto (\mathrm{Int}(\mathcal{C}_i), \mathrm{Ext}(\mathcal{C}_i)),$$

where $(\mathrm{Int}(\mathcal{C}_i), \mathrm{Ext}(\mathcal{C}_i))$ was defined in Section 2. We now have:

THEOREM 4. *The partial Voronoi map $\mathcal{V}$ is Scott continuous and Hausdorff and Lebesgue computable.*

Now assume that the N rectangles $R_i = \{p_i\}$ $(1 \leq i \leq N)$, are actually singletons, and p_i are computable points of $\mathbb{R}^2$ which are approximated by computable sequences of dyadic (or rational) rectangles: $\{p_i\} = \bigcap_{j\geq 0} R_{ij}$. We have the following result.

THEOREM 5. *The N pairs of increasing sequences of open sets $(Int(\mathcal{C}_{ij}))_{j\geq 0}$ and $(Ext(\mathcal{C}_{ij}))_{j\geq 0}$ converge respectively to the classical interior and exterior of the classical Voronoi cell of p_i, which form a maximal element of $\mathbf{S}\mathbb{R}^d$. Moreover, this convergence is effective in the Hausdorff distance and Lebesgue measure.*

6. REFERENCES

[1] F. Aurenhammer and R. Klein. Voronoi diagrams. In J.-R. Sack and J. Urrutia, editors, *Handbook of computational geometry*, pages 201–290. Elsevire Science B.V., 1999.

[2] F. Avnaim, J. D. Boissonnat, O. Devillers, F. Preparata, and M. Yvinec. Evaluation of a new method to compute sign of determinants. In *Proc. Eleventh ACM Symposium on Computational Geometry*, June 1995.

[3] H. Bronimann, J. Emiris, V. Pan, and S. Pion. Computing exact geometric predicates using modular arithmetic with single precision. *ACM Conference on Computational Geometry*, 1997.

[4] H. Brönnimann and M. Yvinec. Efficient exact evaluation of sign of determinants. In *Proc. Thirteenth ACM Symposium on Computational Geometry*, pages 136–173, June 1997.

[5] M. de Berg, M. van Kreveld, M. Overmars, and O. Schwarzkopf. *Computational geometry, algorithms and applications*. Springer, 2nd edition, 2000.

[6] H. Desaulniers and N. F. Stewart. Robustness of numerical methods in geometric computation when problem data is uncertain. *Computer-Aided Design, special issue on uncertainties in geometrical design*, 25(9):539–545, 1993.

[7] O. Devillers, A. Fronville, B. Mourrain, and M. Teillaud. Algebraic methods and arithmetic filtering for exact predicates on circle arcs. In *Proc. Sixteenth ACM Symposium on Computational Geometry*, pages 139–147, June 2000.

[8] A. Edalat. Domains for computation in mathematics, physics and exact real arithmetic. *Bulletin of Symbolic Logic*, 3(4):401–452, 1997.

[9] A. Edalat and A. Lieutier. Foundation of a computable solid modeling. In *Proceedings of the fifth symposium on Solid modeling and applications*, ACM Symposium on Solid Modeling and Applications, pages 278 – 284, 1999.

[10] A. Edalat, A. Lieutier, and E. Kashefi. The convex hull in a new model of computation. In *Proc. 13th Canad. Conf. Comput. Geom.*, pages 93–96, 2001.

[11] A. Edalat and P. Sünderhauf. A domain theoretic approach to computability on the real line. *Theoretical Computer Science*, 210:73–98, 1998.

[12] S. Fortune. Voronoi diagrams and delaunay triangulations. In D.-Z. Du and F. Hwang, editors, *Computing in Euclidean Geometry*, pages 193–233, Singapore, 1992. World Scientific. Lecture notes series on Comput.

[13] S. Fortune. Polyhedral modeling with multi-precision integer arithmetic. *Computer-Aided Design*, 29(2):123–133, 1997.

[14] S. Fortune and C. von Wyk. Efficient exact arithmetic for computational geometry. In *Proceeding of the 9th ACM Annual Symposium on Computational Geometry*, pages 163–172, 1993.

[15] M. Goodrich, L. Guibas, J. Hershberger, and P. TanenBaum. Snap rounding line segments efficiently in two and three dimensions. In *Proc. Thirteenth ACM Symposium on Computational Geometry*, pages 284–293, June 1997.

[16] L. Guibas, D. Salesin, and J. Stolfi. Epsilon geometry - building robust algorithms for imprecise computations. In *Proceeding of the 5th ACM Annual Symposium on Computational Geometry*, pages 208–217, 1989.

[17] C. Y. Hu, T. Maekawa, E. C. Shebrooke, and N. M. Patrikalakis. Robust interval algorithm for curve intersections. *Computer-Aided Design*, 28(6/7):495–506, 1996.

[18] C. Y. Hu, N. M. Patrikalakis, and X. Ye. Robust interval solid modeling, part ii: boundary evaluation. *CAD*, 28:819–830, 1996.

[19] LEDA. `http://www.mpi-sb.mpg.de/LEDA/leda.html`.

[20] V. Milenkovic. Robust polygon modelling. *Computer-Aided Design*, 25(9), September 1993.

[21] Y. Oishi and K. Sugihara. Topology oriented divide-and-conquer algorithm for voroni diagrams. *Computer Vision,Graphics, and Image Processing: Graphical Models and Image Processing*, 57:303–314, 1995.

[22] T. Peters, D. Ferguson, N. Stewart, and P. Fussell. Algorithmic tolerances and semantics in data exchange. *ACM Conference on Computational Geometry*, 1997.

[23] M. B. Pour-El and J. I. Richards. *Computability in Analysis and Physics*. Springer-Verlag, 1988.

[24] F. Preparata and M. Shamos. *Computational Geometry: an introduction*. Springer Verlag, 1985.

[25] T. W. Sederberg and R. T. Farouki. Approximation by interval bezier curves. *IEEE Comput. Graph. Appl.*, 15(2):87–95, 1992.

[26] M. Segal. Using tolerances to guarantee valid polyhedral modeling results. *Computer Graphics*, 24(4):105–114, 1990.

[27] K. Sugihara and M. Iri. A robust topology-oriented incremental algorithm for voroni diagrams. *International Journal of Computational Geometry and Applications*, pages 179–228, 1994.

[28] K. Sugihara, Y. Ooishi, and T. Imai. Topology-oriented approach to robustness and its application to several Voronoi-diagram algorithms. In *Proc. 2nd Canad. Conf. Comput. Geom.*, pages 36–39, 1990.

[29] K. Weihrauch. *Computability*, volume 9 of *EATCS Monographs on Theoretical Computer Science*. Springer-Verlag, 1987.

[30] C. K. Yap. The exact computation paradigm. In D. Z. Du and F. Hwang, editors, *Computing in Euclidean Geometry*. World Scientific, 1995.